# Droplet Velocity Measurement Of Acetone-Water Spray Using Fluorescence-Based Particle Image Velocimetry

Anbarasan Sekar[1,*], Yedhu Krishna[2], Aravind Vaidyanathan[1]

1: Department of Aerospace Engineering, Indian Institute of Space Science and Technology, Thiruvananthapuram - 695547, Kerala, India
2: Specrule Scientific Pvt Ltd, Space Technology Innovation and Incubation Centre, Indian Institute of Space Science and Technology, Thiruvananthapuram - 695547, Kerala, India
*Corresponding author: anbumsr@gmail.com

**Keywords:** Fluorescence-based PIV, Acetone PLIF, Acetone-water mixture.

ABSTRACT

A method for measuring the velocity of liquid droplets emanating from an effervescent injector into ambient air was experimented using a mixture of acetone and water. Conventional methods such as Laser Doppler Velocimetry and Particle Image Velocimetry, which utilise Mie-scattering, have limitations due to multiple scattering and strong surface reflections, respectively. In the current study, we demonstrate fluorescence-based particle image velocimetry, which can overcome the abovementioned difficulty. Unlike previous similar studies that used fluorescent dyes, the inherent fluorescence of acetone is utilised in our strategy. The acetone and water were mixed in different volume ratios, and the effervescent jet was produced with air. The Gas-to-Liquid ratio of 8% was considered in this study. The spray droplets were excited using the fourth harmonic of the Nd-YAG laser. Two acetone Planar Laser laser-induced fluorescence images are acquired with a CCD camera and with a 20 $\mu s$ time difference. The velocity vectors are obtained based on the cross-correlation between the two images. The results showed that absorption greatly influences the estimated velocity distribution. At a low acetone concentration, the velocity distribution became uniform around the jet centre line. A high-intensity laser could improve the velocity estimate in the core of the aerated jet. The proposed method can be applied directly to ambient and pressurised conditions where wall scattering is dominant. The directional independence of the fluorescence is also an advantage in scenarios where the imaging angle is a constraint.

## 1. Introduction

Sprays play a very important role in many applications, such as combustion, medicine, agriculture, and pulverization. Injectors are characterized based on the droplet diameter and the droplet velocities. The droplet velocities depend on the type of injection. Effervescent injectors produce very fine droplets with high velocities. Depending on the aeration levels, liquid droplet velocities can vary significantly. The compressibility of the aeration gas could alter the void fraction and make the analytical estimates highly complex. Experimental measurement of droplet velocity distribution is important for validating computational methods and can also be used for empirical models. Droplet velocities are mainly measured using LDV (Cole & Swords, 1979), and cross-correlation based PIV(Peterson, 2009; Anand et al., 2012; Acharya et al., 2021). For the correlation-based strategy, scattering, shadowgraph, or fluorescence images are used. The LDV technique is highly accurate, but it is a point measurement. The shadowgraph-based PIV is a line-of-sight technique which can not be applied to dense sprays. The PIV technique with Mie-scattering also would not be effective in dense sprays due to the multiple scattering from the droplets outside the laser sheet. The multiple scattering can be removed using SLIPI method but it is usually applied only to droplet sizing measurements (Storch et al., 2016). The fluorescence-based PIV used in the current work also suffers from multiple scattering, but it is less severe than the scattering method. Since the scattering intensity is proportional to the droplet surface area and the fluorescence is proportional to the volume of the droplet, the scattering of illumination wavelength and the fluorescence from small droplets outside the laser sheet should be low. If the droplets show strong absorption this effect will be further reduced. Even though the scattered light produces additional fluorescence from the droplets outside the laser sheet, the fluorescence signal is proportional to the intensity of the scattered light. For the fluorescence-based PIV, mostly Rhodamine (Moon et al., 2010) and DCM dyes(Sepret, 2010) were used as tracers due to the fact that these dyes could be easily excited with 532 nm wavelength from the Nd-YAG laser.

The current study utilizes the fluorescence from the acetone-water mixture for the PIV technique. Acetone is completely miscible in water and may react to produce Geminal diol with the equilibrium constant in the order of $10^{-3}$, which is negligible. As a result of its high state density, acetone exhibits continuous and broad absorption spectra, beginning at around 225 nm and ending at around 320 nm, with maximum absorption occurring at around 275 nm. Additionally, the utilization of the fourth harmonic of the Nd-YAG laser (266 nm) can be advantageous for exciting the acetone molecules. When acetone is excited with a wavelength of 266 nm, its fluorescence covers a wide range of wavelengths, from 300 nm to 500 nm(Lozano et al., 1992).

The current study aims to obtain droplet velocity distribution of an aerated jet using fluorescence from a readily available substance with low cost, and with low health hazard. The reason for using fluorescence signal for PIV is that the signal is less affected by the multiple scattering. Acetone is chosen as the fluorescent agent because it is readily miscible in water, and the fluorescence spectrum extends to the visible spectrum, which is an advantage in terms of the typical cameras used in PIV applications. Four different volume percentages of acetone were considered to study the effects of acetone percentage on the droplet velocity distribution.

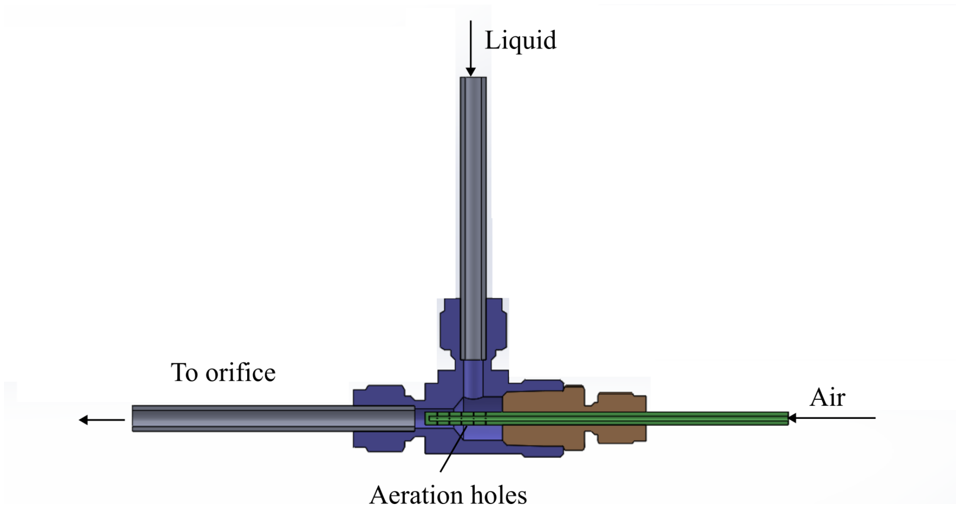


**Figure 1.** Cross-sectional view of the injector assembly

## 2. Experimental methodology

The injection system comprises an injector with an inside-out configuration for the aeration, two pressure regulators, an acetone-water mixture tank for the liquid line, and two mass flow controllers for controlling the liquid and the airflow rates. A total of 20 aeration holes with the size of 250 $\mu m$ were distributed uniformly in the axial and circumferential directions. The holes were manufactured using the EDM process. The cross-sectional view of the assembly design of the injector is shown in Fig. 1. Four different acetone and water mixtures were tested with a volume ratio of 25%, 50%, 75%, and 100%. Both lines received air from a reservoir at a maximum pressure of 10 bar. The mass flow controllers automatically adjusted the upstream pressure of the aeration gas and liquid to maintain the desired mass flow rate. The mass flow rate of the liquid and air were fixed at 2 $g/s$ and 0.16 $g/s$, respectively. These flow rates correspond to a GLR of 8%. The two lines were merged around 80 mm upstream of the injector exit. The schematic of the setup is given in Fig. 2.

A double pulsed Nd-YAG laser (Quanta-Ray® PIV 400) was operated in the fourth harmonic mode and the timing of the laser pulses were controlled externally to synchronize the pulses with camera frames. The limitation of this method is the time interval between the two laser pulses based on the phosphorescence lifetime, which refers to the duration of electrically excited molecules in the triplet state. According to a study by Tran et al. (2006), the phosphorescence lifetime of liquid acetone is around 1 $\mu$s. The scattering of 266 nm and the residue of 532 nm from the laser were cut off by 305 nm long-pass and 500 nm short-pass filters, respectively. The CCD camera, model PCO 2000, was fitted with an 80 - 200 mm zoom lens, which captures sufficient fluorescence signal from the high-concentration liquid mixture. Even though the filters allow wavelengths from 305 nm to 500 nm, the lens system allows only the visible spectrum. Since the quantum

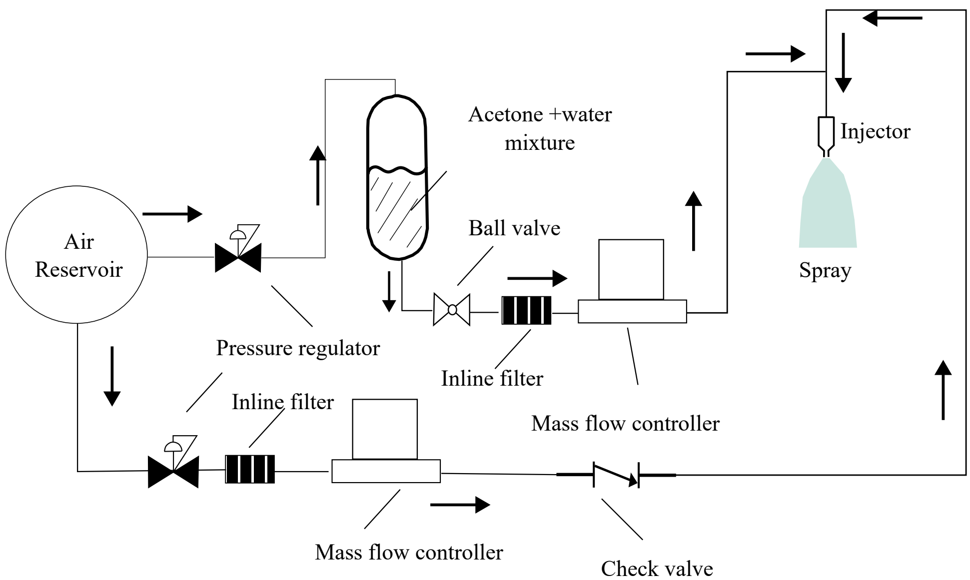


**Figure 2.** Schematic of the overall experimental setup

efficiency of the camera is also low in the UV range, the signal collected was effectively a partial amount of the original signal. The fluorescence signal acquired from the droplet of the liquid mixture would be sufficient for the CCD camera, even at an excitation energy of 40 mJ. The camera was utilized in double shutter mode, and the frames were synchronized with laser pulses using a BNC™ delay/pulse generator. The time interval of 20 $\mu$s between each laser pulse was kept for the current magnification. Figure 3 displays the diagram of the experimental configuration.

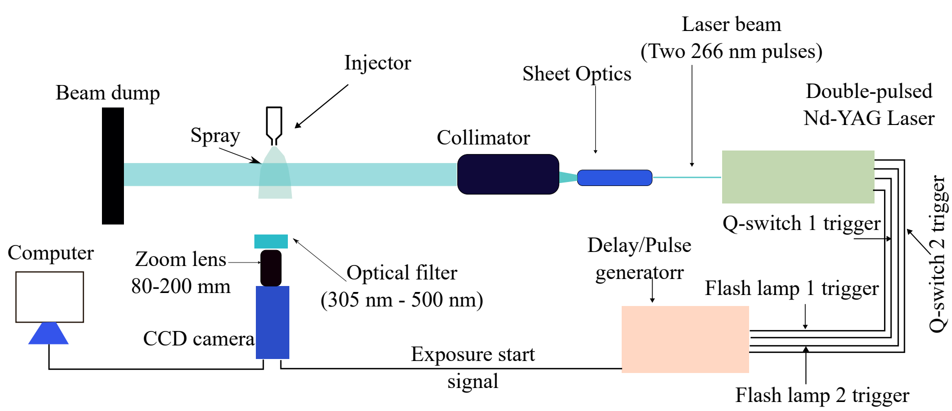


**Figure 3.** Schematic of the fluorescence-based PIV setup

A calibration plate with two levels was utilized for spatial calibration. The velocity vectors were acquired using the cross-correlation technique with Davis 10.1. The frames, which had a resolution of 2048 x 2048 pixels$^2$, were partitioned into interrogation windows measuring 24 x 24 pixels$^2$ for the final pass. The determination of velocity vector uncertainties is established by utilizing the cross-correlation peak, standard deviation, and sample size employed in calculating mean velocity (Sciacchitano & Wieneke, 2016).

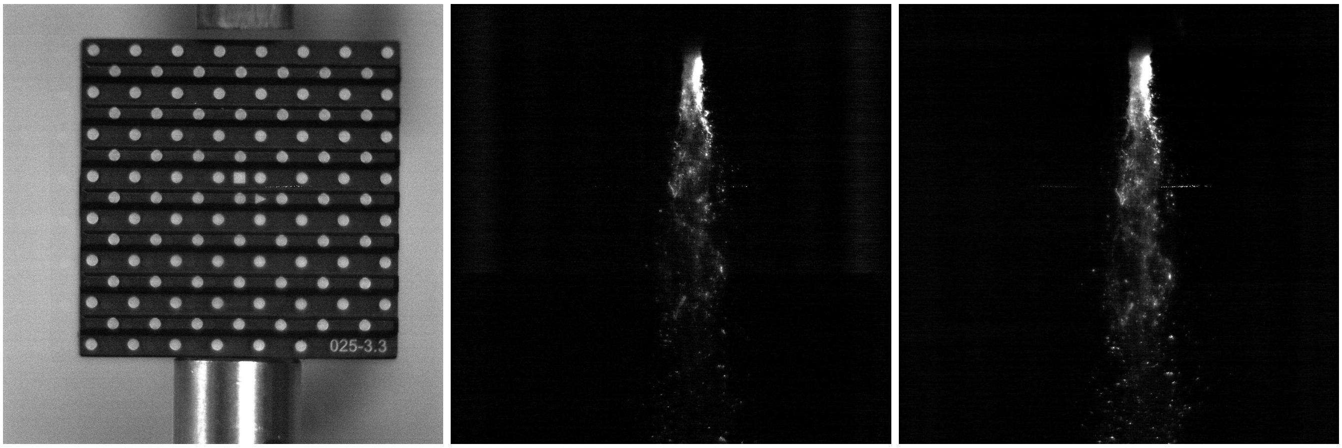


(a) Calibration plate (b) Frame 1 (c) Frame 2

**Figure 4.** Raw images obtained from the experiment with pure acetone jet

## 3. Results and discussion

The experiments were conducted for the acetone-water mixture spray with a GLR of 8%, and the results are presented in this section. Figure 4 displays the raw images obtained from the experiment. The calibration yields a spatial resolution of 59.22 pixels/mm. The second frame was exposed in the order of milliseconds depending on the readout time and the frame rate. These raw fluorescence images did not exhibit any streaks, which indicates a fast decay of phosphorescence and the suitability of acetone as a fluorescent tracer in PIV applications.

The fluorescence-based PIV results are given in Fig. 5 for different acetone concentrations. Even though the droplet velocity clearly shows the annular nature of the spray, the velocity should be higher in the core of the jet. The pattern obtained in this contour was due to the fact that the fluorescence signal is proportional to the volume of the droplets since the concentration is constant. This produced a low signal in the core of the jet, which caused the velocity to bias towards a large droplet region. In the pure acetone case, there was a clear asymmetry about the center line due to the strong absorption of the laser sheet by the acetone droplets. When the acetone concentration was reduced, the effect absorption effects became minimal, and the symmetry in the droplet velocities could be seen. A low-velocity patch on the right side of the center line was due to the saturated pixels in the camera, which could be seen from the raw images shown previously.

To compare the velocity profile at different distances along the jet direction, three lines were considered at $y/d = -10$, $y/d = -20$, and $y/d = -30$. These are marked with yellow dashed lines in Fig. 5a. The velocity profiles along these lines for different acetone percentages are shown in Fig. 6. As seen from the velocity contour of the pure acetone jet, the velocity on the left side of the center line showed lower velocity at all locations. When the acetone percentage was reduced, the velocity variation became more symmetric as well as the dip in the central portion of the jet was reduced.

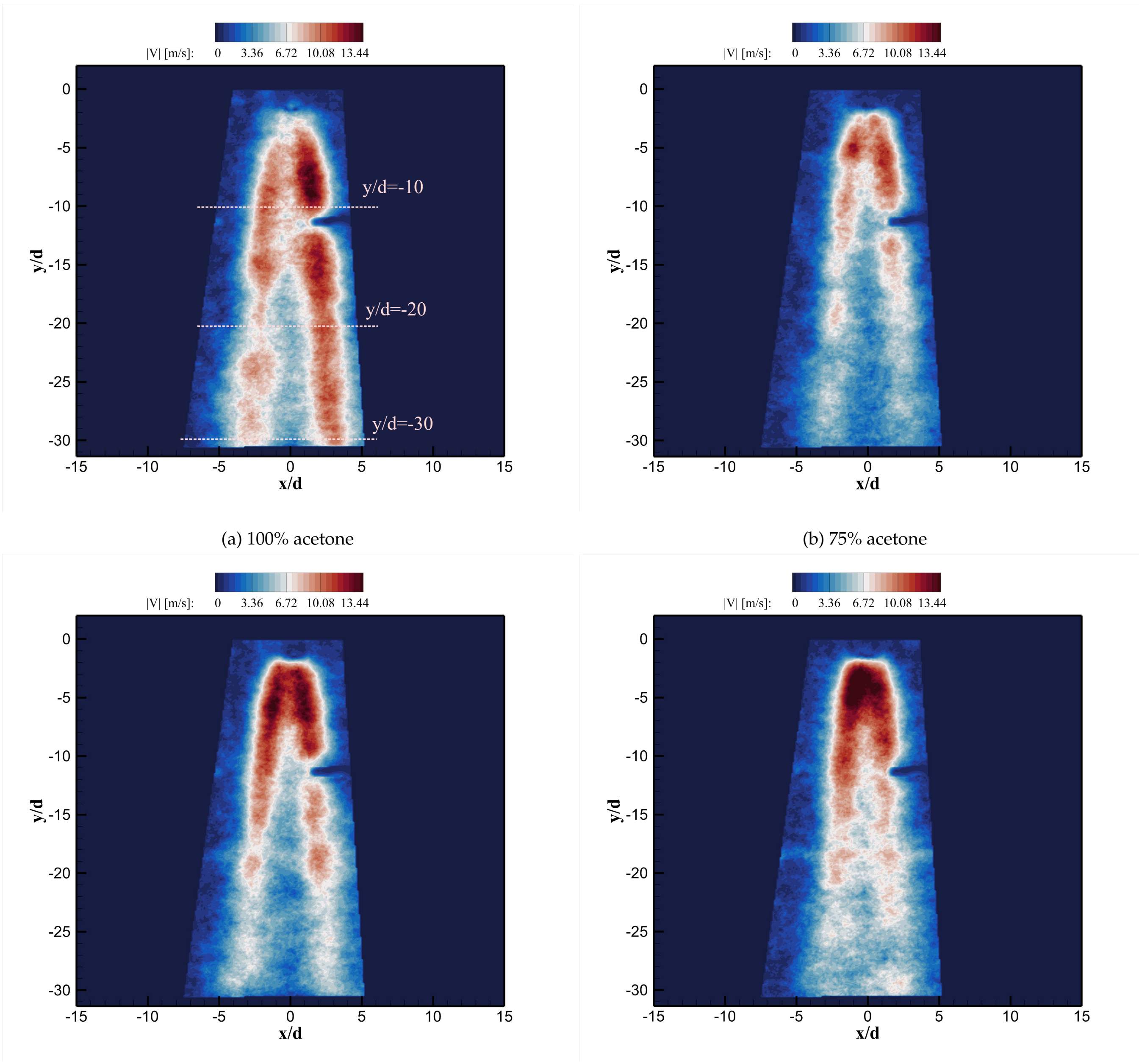


(a) 100% acetone

(b) 75% acetone

(c) 50% acetone

(d) 25% acetone

**Figure 5.** Contour of droplet velocity for different acetone percentage

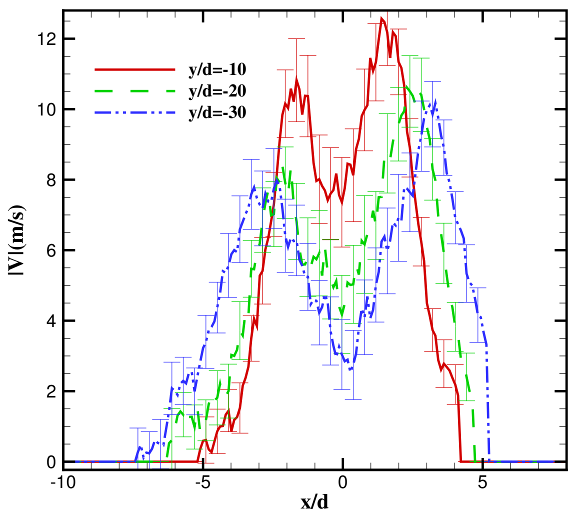


(a) 100% acetone

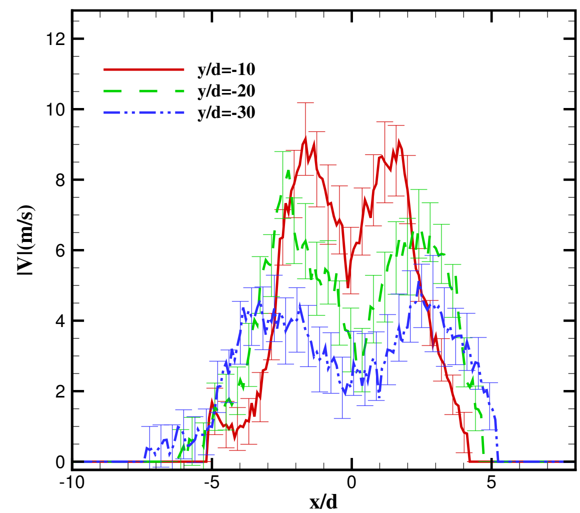


(b) 75% acetone

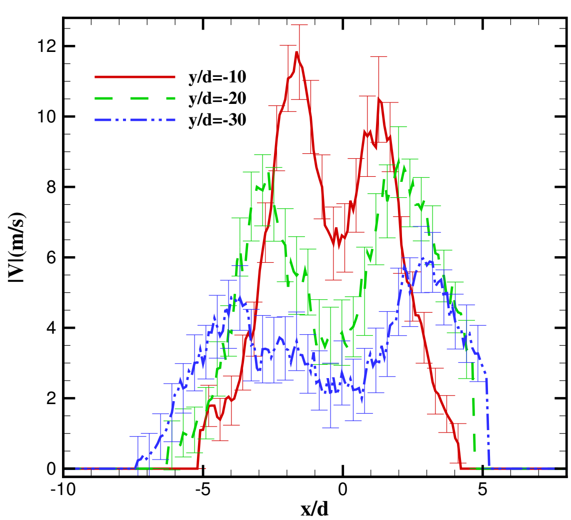


(c) 50% acetone

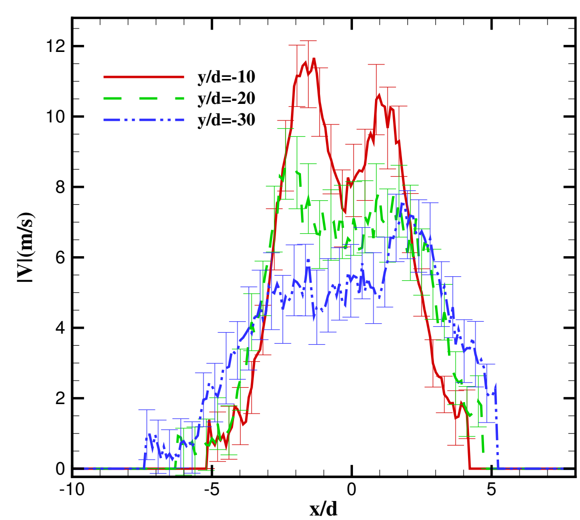


(d) 25% acetone

**Figure 6.** Comparison of velocity profiles at different locations for different acetone percentage

With reduced acetone concentration, the fluorescence signal in the low-liquid-density regions become even lower and this affects the signal levels. The difference in the velocity profiles among different acetone percentages could have also occurred due to the variation of mixture properties such as density, viscosity, and surface tension. The water and acetone show considerable differences in the surface tension, which affects the $We$ of the liquid jet.

The measurements were carried out with an energy of 40 mJ/pulse which can be increased to improve the fluorescence signal from the core of the aerated jet. The concentration and laser energy can be thus optimized to use the maximum dynamic range of the camera. This would improve estimate of the velocity distribution in the core regions. The lens system which allows ultraviolet could be implemented to improve the signal strength since the sensitivity of most CCD cameras extends up to 300 nm. The PIV cameras usually have high pixel resolution and binning could also be implemented to improve the SNR. In a stereoscopic PIV measurement where the cameras are placed in forward-backward scattering configuration, the signal levels are different in each camera with similar lens setup. In such scenarios this method could be implemented due to the directional independence of the fluorescence.

## 4. Conclusions

Fluorescence-based PIV measurements were carried out for an aerated jet with an acetone-water mixture and air and with a GLR of 8%. The effects of different acetone percentages were also examined in this study. The following conclusions were drawn from the results.

- The reduced multiple scattering effects in this method can improve the velocity estimation of dense sprays. The conventional PIV systems can be directly used with a few additional components for this method.
- PIV results obtained using fluorescence were affected by the strong absorption of pure acetone jet.Asymmetry in the velocity distribution was observed for the pure acetone jet. When the acetone percentage was reduced, the effect became low.
- Since the fluorescence signal in sprays depends on the volume of the droplet, the velocity distribution in the core of the aerated jet was greatly affected.
- This method can also be applied to sprays inside wind tunnels and pressurized chambers where the wall scattering is a problem. The problem of dyes sticking to the surfaces also could be avoided in this method. Compared to the available fluorescent tracers, acetone has many advantages, such as availability, cost, and low health hazards.

**Nomenclature**

| | |
|---|---|
| $d$ | Exit diameter of the injector [mm] |
| $x, y$ | Lateral, and axial directions of the jet, respectively |
| $\|V\|$ | Droplet velocity magnitude [m/s] |
| $We$ | Weber number |
| **Abbreviations** | |
| $CCD$ | Charged-coupled device |
| $EDM$ | Electric Discharge Machining |
| $GLR$ | Gas-to-Liquid ratio |
| $LDV$ | Laser Doppler Velocimetry |
| $PIV$ | Particle Image Velocimetry |
| $SLIPI$ | Structured Laser Illumination Planar Imaging |
| $SNR$ | Signal-to-Noise ratio |

**References**


Acharya, A. S., Lowe, K. T., & Ng, W. F. (2021). Fluorescent piv using atomized liquid particles. In *14th international symposium on particle image velocimetry* (Vol. 1).

Anand, T., Madan Mohan, A., & Ravikrishna, R. (2012). Spray characterization of gasoline-ethanol blends from a multi-hole port fuel injector. *Fuel*, *102*, 613-623. (Special Section: ACS Clean Coal)

Cole, J., & Swords, M. (1979). Laser doppler anemometry measurements in an engine. *Applied Optics*, *18*(10), 1539–1545.

Lozano, A., Yip, B., & Hanson, R. (1992). Acetone: a tracer for concentration measurements in gaseous flows by planar laser-induced fluorescence. *Experiments in fluids*, *13*(6), 369–376.

Moon, S., Matsumoto, Y., Nishida, K., & Gao, J. (2010). Gas entrainment characteristics of diesel spray injected by a group-hole nozzle. *Fuel*, *89*(11), 3287-3299.

Peterson, S. V., B. (2009). Simultaneous flow field and fuel concentration imaging at 4.8 khz in an operating engine. *Applied Physics B*, *97*, 887–895.

Sciacchitano, A., & Wieneke, B. (2016). Piv uncertainty propagation. *Measurement Science and Technology*, *27*(8), 084006.

Sepret, B. R. M. M. C. G., V. (2010). Effect of ambient density and orifice diameter on gas entrainment by a single-hole diesel spray. *Experiments in Fluids*, *49*(6), 1293-1305.

Storch, M., Mishra, Y. N., Koegl, M., Kristensson, E., Will, S., Zigan, L., & Berrocal, E. (2016). Two-phase slipi for instantaneous lif and mie imaging of transient fuel sprays. *Optics Letters*, *41*(23), 5422–5425.

Tran, T., Kochar, Y., & Seitzman, J. (2006). Measurement of acetone fluorescence and phosphorescence at high presssures and temperatures. In *44th aiaa aerospace sciences meeting and exhibit.*